ELSEVIER

Materials Science and Engineering A252 (1998) 85–92

MATERIALS SCIENCE & ENGINEERING A

Low-cycle fatigue behaviors of commercial-purity titanium

Z.F. Zhang [a,b,*], H.C. Gu [b], X.L. Tan [b]

[a] *State Key Laboratory for Fatigue and Fracture of Materials, Institute of Metal Research, Academia Sinica, 72 Wenhua Road, Shenyang 110015, People's Republic of China*

[b] *Xi'an Jiaotong University, Xi'an 710049, People's Republic of China*

Received 29 November 1997; received in revised form 2 March 1998

Abstract

Low-cycle fatigue behaviors of commercial-purity titanium (TA2) were investigated under constant total strain amplitude control at room temperature in air. It was found that commercial-purity titanium exhibited a complex cyclic hardening behavior over the strain range 0.5–2.4%. By optical microscope (OM) and Image Scan Analyzer, the cyclic deformation twins were observed and the quantitative relations of twin fraction F_T versus strain amplitudes and cyclic numbers were proposed. Meanwhile, the dislocation structures in cyclically deformed commercial-purity titanium were observed by transmission electron microscopy (TEM). In combining the observations of dislocation patterns and deformation twins, a microstructure evolution map was given. On the basis of the experimental results, the effect of microstructures (including deformation twins and dislocation patterns) on the cyclic stress–strain response was discussed.

Keywords: Commercial-purity titanium; Cyclic deformation; Deformation twin; Dislocation patterns

1. Introduction

During the last 30 years, the cyclic deformation behaviors of copper single crystals and polycrystals have been well documented [1–4]. However, titanium, having another type of lattice structure—hexagonal-close-packed (h.c.p.) metal—is understood insufficiently. Titanium is one of some 20 hexagonal metals, and has two principal virtues: (i) a high strength/weight ratio, and (ii) good corrosion resistance. Due to their excellent properties, titanium and its alloys have been widely applied in industry. At present, almost all the available studies on the fatigue behavior of titanium have been conducted on titanium polycrystals with different grain sizes [5–14]. Only very limited works on the cyclic deformation of titanium single crystal [15,16] and titanium bicrystal [17] can be found, owing to the difficulty of titanium crystal preparation. It is generally believed that, in h.c.p. metals, deformation twinning, as one of the two principal modes of plastic deformation, plays a more important role than it does in cubic metals. Six different twinning systems have been reported in titanium under monotonic and cyclic loading [11,15–25]. Moreover, the basal, prismatic and pyramidal planes often become the slip plane [22,23,25]. Due to the complex slip systems and twinning systems in titanium, the cyclic deformation behaviors of titanium will be more complicated. Consequently, the fatigue mechanism of titanium will be markedly different from that of f.c.c. metals. In this paper, in order to further reveal the cyclic deformation mechanisms of titanium and other h.c.p. metals, on the basis of studies on titanium single crystals [15,16], bicrystals [17] and commercial-purity zirconium [24,26], the low-cycle fatigue behaviors of commercial-purity titanium polycrystal will be investigated.

2. Experimental procedure

Commercial-purity titanium, TA2, was machined to fatigue specimens having a gauge size of $15 \times \Phi 8$ mm. The chemical contents of the material are listed in Table 1. After annealing at 750°C for 2 h under 10^{-5}

* Corresponding author.

0921-5093/98/$19.00
PII S0921-5093(98)00650-9

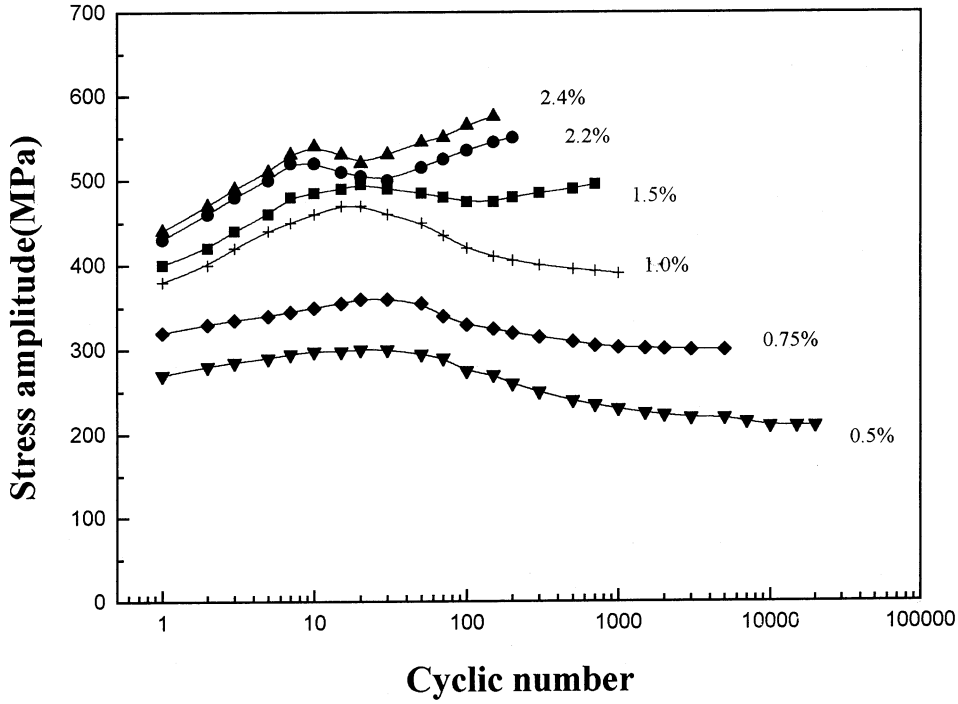

Fig. 1. Cyclic hardening curves of commercial-purity titanium.

Table 1
The chemical contents of commercial purity titanium

Element	Fe	Si	C	N	O	Ti
Content (%)	0.30	0.15	0.05	0.015	0.20	Other

torr in vacuum, an α-Ti structure with the equiaxed grains about 35 μm and few annealing twins was obtained. Cyclic deformation was performed on a Schenck servo-hydraulic machine under constant totaly strain amplitude control at room temperature in air. A triangular waveform with a constant strain rate of 4×10^{-3} s^{-1} was used. The peak push, pull loads and hysteresis loops were recorded automatically by computer. The selected total strain amplitudes were 0.5, 0.75, 1.0, 1.5, 2.2 and 2.4%, respectively. At each strain amplitude, a group of specimens were cycled to some different cycles, N_i, and stopped for observation of deformation twins and dislocations. After cyclic deformation, these specimens were spark-cut from the gauge sites. The specimens were then polished and etched with a solution of 45%H_2O, 45%HNO_3 and 10%HF. By optical microscopy (OM), the deformation twins within the fatigued specimens were observed and the twin fraction, F_T, was measured by an Image Scan Analyzer. In the end, the dislocation structures of commercial-purity titanium at different strain amplitudes and cycles were observed using a JEM-200CX transmission electron microscope (TEM).

3. Results

3.1. Cyclic stress–strain responses

Commercial-purity titanium exhibited a relatively complex cyclic hardening behavior at the selected strain amplitudes. The cyclic hardening curves at different strain amplitudes are shown in Fig. 1. At relatively lower strain amplitudes ($\varepsilon_a = 0.5$, 0.75, 1.0%), after initial cyclic hardening, cyclic softening occurred until

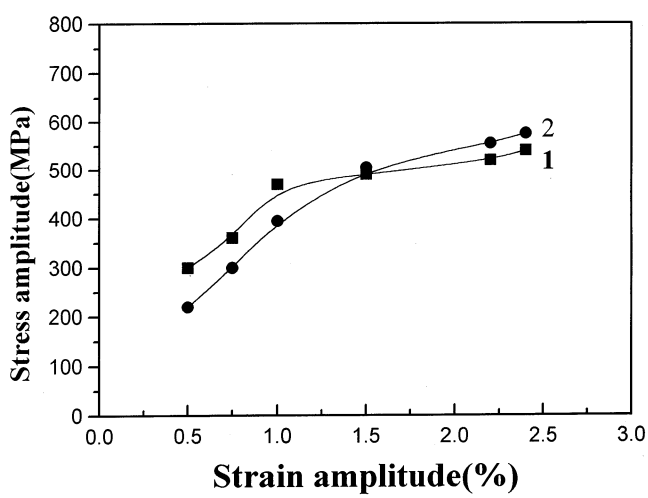

Fig. 2. Cyclic stress–strain curves of commercial-purity titanium. Curve 1 was plotted as the initial maximum cyclic stress vs. strain amplitude; curve 2 was plotted as the secondary cyclic hardening maximum stress vs. strain amplitude.

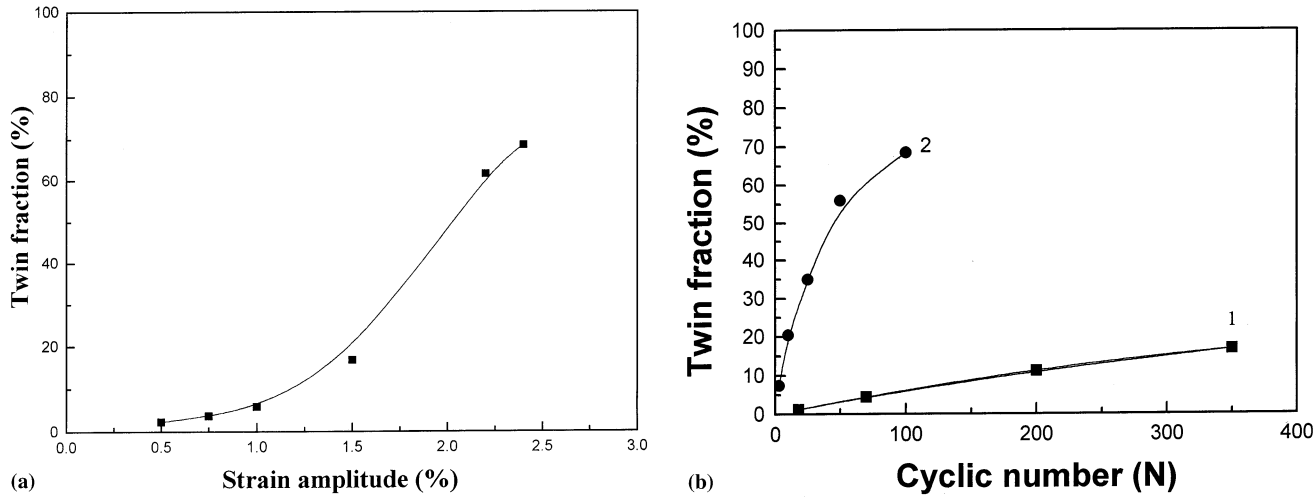

Fig. 3. The relations of twin fraction vs. strain amplitude and cyclic number: (a) the relation of twin fraction vs. strain amplitude, where the twin fraction was measured from the failed specimens; (b) the evolution of deformation twins at strain amplitudes of 1.5 and 2.4%.

fracture. At medium strain amplitude ($\varepsilon_a = 1.5\%$), the cyclic stress amplitude changed little after initial cyclic hardening and showed a cyclic saturation behavior. However, at relatively higher strain amplitudes ($\varepsilon_a =$ 2.2, 2.4%), an obviously secondary cyclic hardening occurred after initial cyclic hardening and consequent cyclic softening. The stress amplitude caused by secondary hardening is obviously higher than that caused by initial cyclic hardening. This cyclic hardening behavior is very similar to the previous results [5–10]. Meanwhile, it is found that the plastic strain amplitude decreased as the stress amplitude increased during cyclic hardening. The cyclic stress–strain curves of commercial-purity titanium are shown in Fig. 2. Because there is no obvious cyclic saturation at most of the selected strain amplitudes except that of 1.5%, both the maximum stress amplitude caused by initial (curve 1) and secondary (curve 2) cyclic hardening are selected. The results showed that the cyclic stress increased rapidly at the low strain range with increasing strain amplitude and the stress increased slowly at the higher strain range.

4. Observation of deformation twins

As the specimens failed, the deformation twins within commercial-purity titanium and their fraction, F_T, were observed and measured. The quantitative relations of twin fraction F_T versus strain amplitude and cyclic number are shown in Fig. 3. Fig. 3(a) shows that the twin fraction increases with increasing strain amplitude within the fractured specimens even though the fatigue lives of those specimens are very short at higher strain amplitude. At relatively higher strain amplitudes (1.5 and 2.4%), the quantitative relations of twin fraction versus cyclic number were proposed (see Fig. 3(b)). It can be seen that the twin fraction F_T increases almost linearly with the cyclic number at the strain amplitude of 1.5% (see curve 1 in Fig. 3(b)). When the strain amplitude was increased to 2.4%, however, after an initial linear increase with the cyclic number, the twin fraction F_T increased slowly with further cyclic deformation (see curve 2 in Fig. 3(b)). Meanwhile, it is found that the size of the deformation twin is nearly the same at the same strain amplitude, but the greater the applied strain amplitude, the larger is the size of the deformation twin. In Fig. 4(a)–(d), the deformation twins within the specimens cyclically deformed at a strain amplitude of 2.4% are shown.

4.1. Observation of dislocation pattern

The TEM observation results showed that the dislocation structures at all strain amplitudes are dislocation dipoles and multi-dipoles at the start of cyclic deformation, as shown in Fig. 5(a)–(c). At relatively lower strain amplitudes ($\varepsilon_a = 0.5$, 0.75%), the dislocation density increases and the dislocation dipoles become the dislocation tangles until fracture (see Fig. 6). With increasing strain amplitude ($\varepsilon_a = 1.0$, 1.5%), irregular dislocation walls and dislocation cells can be observed during cyclic deformation, as indicated in Fig. 7. At relatively higher strain amplitudes ($\varepsilon_a = 2.2$, 2.4%), the dislocation density increased rapidly during initial cyclic hardening and the microstructure evolved into higher dislocation density regions as those specimens fractured, as shown in Fig. 8. The dislocation structures observed at all the strain amplitudes are obviously different those in cyclically deformed polycrystalline copper, in which persistent slip bands (PSBs) and some labyrinth structures [27,28] can often be observed. Based on many observations of dislocation structures

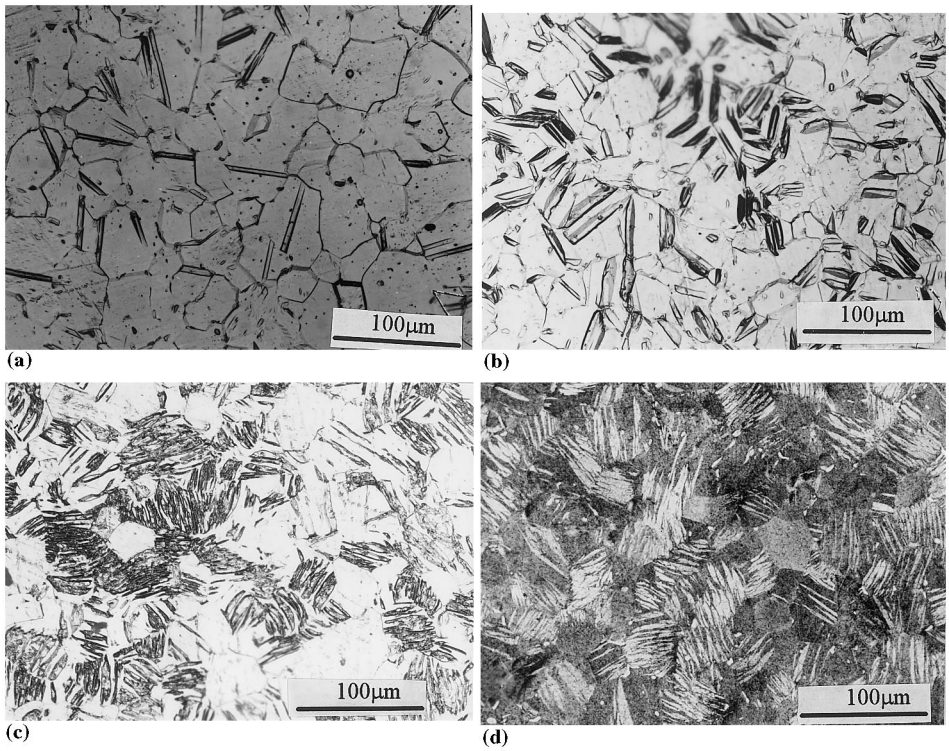

Fig. 4. Deformation twins within the specimens fatigued at a strain amplitude of 2.4%: (a) $N = 3$ cycles; (b) $N = 10$ cycles; (c) $N = 50$ cycles; (d) $N = 100$ cycles.

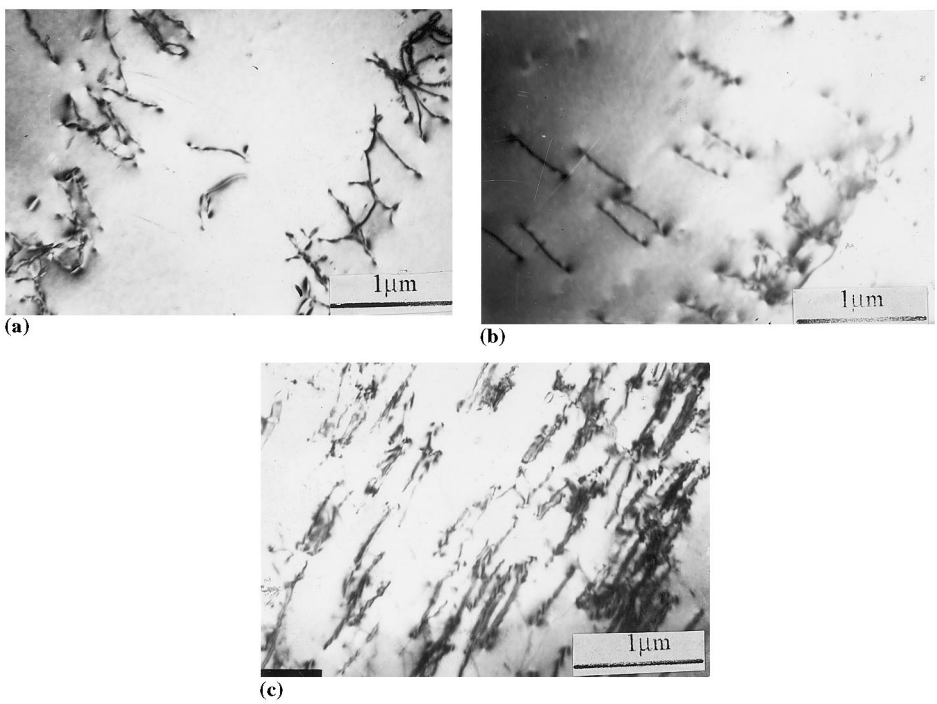

Fig. 5. Dislocation dipoles within the specimens cyclically deformed at lower strain amplitudes (0.5, 0.75 and 1.0%) during initial cyclic hardening: (a) $\varepsilon_a = 0.5\%$ ($N = 20$ cycles); (b) $\varepsilon_a = 0.75\%$ ($N = 10$ cycles); (c) $\varepsilon_a = 1.0\%$ ($N = 10$ cycles).

at all the strain amplitudes and different cycles, a microstructure evolution map is given in Fig. 9. It can be seen that regions (a)–(d) correspond to different dislocation patterns, line 1 being the curve of fatigue life versus strain amplitude. It is indicated that the dislocation patterns in cyclically deformed commercial-purity titanium are associated with the applied strain amplitude and cyclic number.

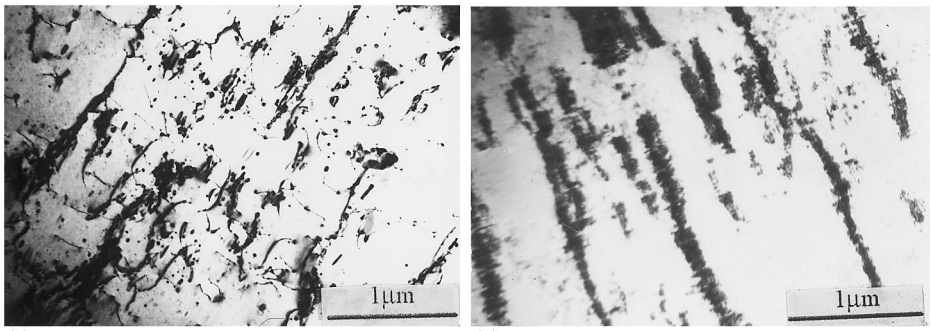

Fig. 6. Dislocation tangles within the specimens after failure: (a) $\varepsilon_a = 0.5\%$ ($N_f = 20600$ cycles); (b) $\varepsilon_a = 0.75\%$ ($N_f = 6000$ cycles).

5. Discussion

5.1. The effect of cyclic deformation on twinning

Titanium, as one of the h.c.p. metallic crystals, has complicated slip and twinning systems. In general, the prismatic plane {1010}, pyramidal plane {1011} and basal plane (0001) are the dominant slip planes. Furthermore, the first-order pyramidal plane {1011} and the second-order pyramidal plane {1122} with a $(c+a)$ Burgers vector are available [22,23]. On the other hand, it is also believed that twinning deformation in titanium plays a more important role than that in cubic metals. In Table 2, the six principal twining systems are listed [11,15–17,25]. Since only a few slip systems can be activated in commercial-purity titanium, twinning deformation often plays an important role, especially at temperatures below 300°C.

Meanwhile, it is known that large strain, high strain rate, low temperature and large grain size will preferentially initiate deformation twins under monotonic loading [5–7,12,13]; however, few references can be found concerning the quantitative relation of twinning with cyclic deformation. From the results above (see Fig. 3), it is known that both the strain amplitude and the cyclic number have an effect on the nucleation of twinning. In general, it was reported that the nucleation of deformation twins requires a critical strain value which decreases with increasing grain size [12,13]. Thus, it might be the reason why few twins can be observed when the strain amplitude is below 1.0%. When the strain amplitude is higher than 1.5%, the critical strain value of nucleating deformation twins may be reached. Consequently, cyclic numbers will also become a relatively important factor in the formation of deformation twins. From Fig. 3(b), the initiation rates of twin fraction F_T at relatively higher strain amplitudes (1.5 and 2.4%) are calculated, respectively, as:

$$\frac{dF_T}{dN} = 0.05\% \quad (\varepsilon_a = 1.5\%) \tag{1}$$

and

$$\frac{dF_T}{dN} = \frac{(1-F_T)^2}{40} \quad (\varepsilon_a = 2.4\%) \tag{2}$$

5.2. Effect of microstructure evolution on cyclic stress–strain responses

The cyclic stress–strain responses of copper single crystal and polycrystals have been well understood. It is well known that there is a plateau region in the cyclic stress–strain curve (CSSC) of copper single crystal and some copper polycrystals [1–4]. Because of the difference lattice structures in copper and titanium, in this study, the cyclic stress–strain response of titanium was somewhat different from that of copper. Firstly, no obvious cyclic saturation was observed, except at the strain amplitude of 1.5%. Secondly, the relatively complex cyclic hardening and cyclic softening processes were observed and no clearly plateau region was found in its cyclic stress–strain curve (CSSC). The results are in good agreement with the results reported by Refs. [5–10].

By observing the microstructure (dislocations and twins) evolution, it can be concluded that the initial cyclic hardening behavior should be attributed to the increase of dislocation density, as shown in Fig. 5. With the increase of the dislocation density within the initial cyclic hardened specimens, the cyclic stress amplitude will be increased continuously. As the dislocation density is accumulated sufficiently, dislocation annihilation will occur. Consequently, the continuous cyclic softening should be associated with dislocation annihilation in the specimens cyclically deformed at low strain amplitudes (0.5, 0.75 and 1.0%). With increasing strain amplitude, twinning will also play a more important role than at low strain amplitude. Deformation twinning may reduce the internal stress concentration and facilitate further deformation. Therefore, the cyclic plastic deformation will become easier as deformation

twins are nucleated. As shown in Fig. 1, when the cyclic number was in the range 10–30 at strain amplitudes of 2.2 and 2.4%, cyclic softening consequently occurred. It may be attributed to the nucleation of deformation twinning. With further cyclic deformation, the fraction of deformation twins increased continuously at higher strain amplitude, as shown in Fig. 3(b). On the one hand, the interactions among deformation twins will restrain the nucleation of new deformation twins, so that cyclic plastic deformation will become more difficult again. On the other hand, the existence of many deformation twins will reduce the average grain size. Thus, it can be postulated that the secondary cyclic hardening should be associated with the formation of a large number of deformation twins within the specimens cyclically deformed at strain amplitudes of 2.2 and 2.4%.

From the evolution map of the microstructures (dislocations and twins), the role of microstructures at different strain amplitudes and cyclic numbers on the cyclic stress–strain response will be revealed. Due to the complex slip systems and twinning systems in titanium, the microstructures caused by cyclic deformation will be different from those in f.c.c. metals, such as copper. Most of the cyclic plastic strains in copper are carried by the persistent slip bands (PSBs) over a certain strain range and a plateau behavior in its CSS curve was often observed [1–4]. However, slipping and twinning play different roles at lower and higher strain ranges during cyclic deformation. Thus, rela-

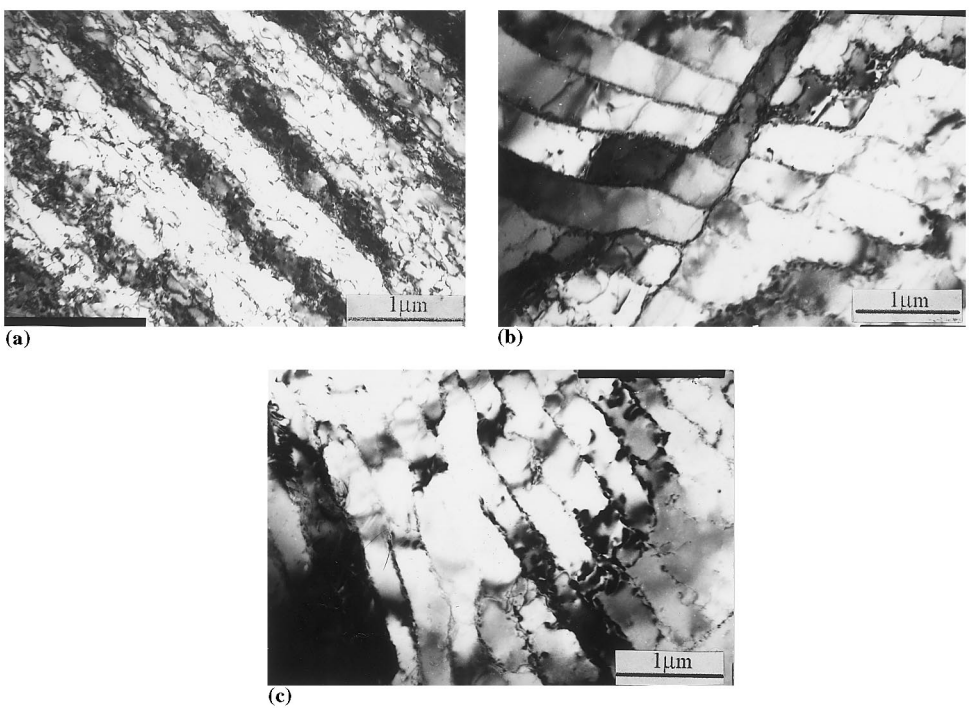

Fig. 7. Irregular dislocation walls and cells within the specimens fatigued at mediate strain amplitudes of 1.0 and 1.5%: (a) $\varepsilon_a = 1.0\%$ ($N = 180$ cycles); (b) $\varepsilon_a = 1.0\%$ ($N = 980$ cycles); (c) $\varepsilon_a = 1.5\%$ ($N = 350$ cycles).

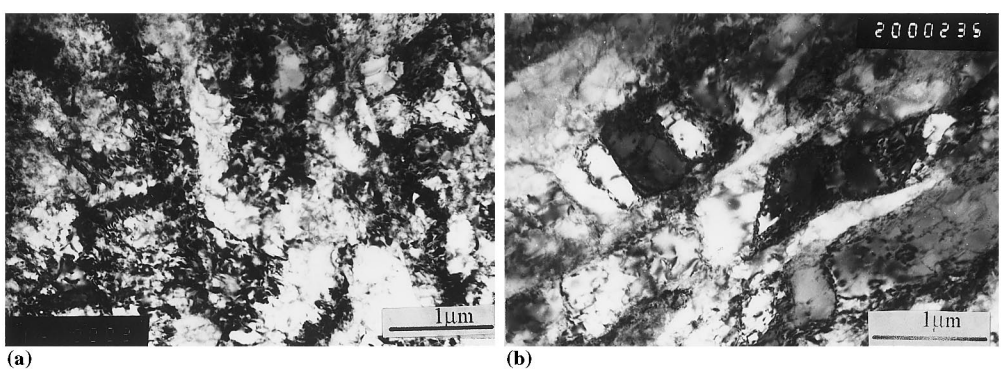

Fig. 8. High dislocation density within the specimens fatigued at a higher strain amplitude of 2.4%: (a) $N = 50$ cycles; (b) $N = 100$ cycles.

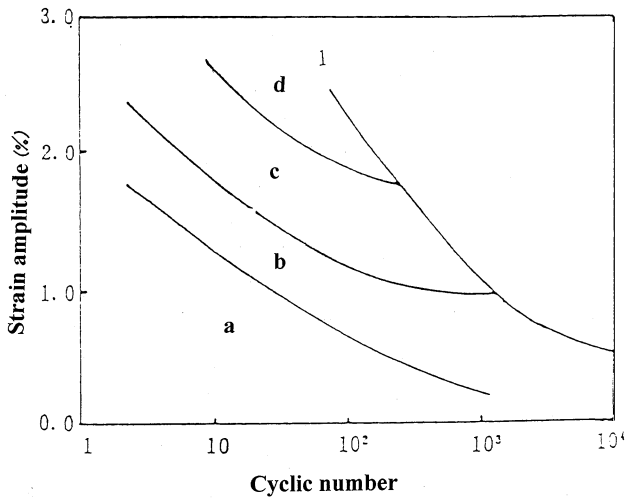

Fig. 9. Evolution map of dislocations and deformation twins in commercial-purity titanium: (a) dislocation dipoles and multi-dipoles; (b) dislocation tangles; (c) dislocation walls and dislocation cells; (d) deformation twins.

tively complex cyclic hardening and cyclic softening processes in commercial-purity titanium were shown (see Fig. 1). As discussed above, it is indicated that the cyclic stress–strain responses of commercial-purity titanium will be affected by dislocation evolution at lower strain amplitudes and by both deformation twin and dislocation evolutions at higher strain amplitudes.

6. Summary and conclusions

From the discussion above, the following conclusions can be drawn:

1. Commercial-purity titanium showed relatively complex cyclic hardening and softening processes, with no obvious cyclic saturation being observed except at a strain amplitude of 1.5%.

Table 2
Six twinning systems in α-Ti

K_1	K_2	η_1	η_2	S
$\{1\,0\,\bar{1}1\}$	$\{10\,\bar{1}3\}$	$\langle 10\,\bar{1}2\rangle$	$\langle 30\,\bar{3}2\rangle$	0.105
$\{10\,\bar{1}2\}$	$\{10\,\bar{1}2\}$	$\langle 10\,\bar{1}1\rangle$	$\langle 10\,\bar{1}1\rangle$	0.167
$\{11\,\bar{2}2\}$	$\{11\,\bar{2}4\}$	$\langle 11\,\bar{2}3\rangle$	$\langle 2\,2\,\bar{4}3\rangle$	0.225
$\{11\,\bar{2}4\}$	$\{11\,\bar{2}2\}$	$\langle 11\,\bar{2}1\rangle$	$\langle 1\,1\,\bar{2}3\rangle$	0.254
$\{11\,\bar{2}3\}$	$\{11\,\bar{2}5\}$	$\langle 33\,\bar{6}2\rangle$	$\langle 5\,5\,10\,2\rangle$	0.533
$\{11\,\bar{2}1\}$	$\{0001\}$	$\langle 11\,\bar{2}6\rangle$	$\langle 1\,1\,\bar{2}\,0\rangle$	0.638

K_1, the twinning plane; K_2, the second undistorted plane; η_1, the twinning direction; η_2, the line of interaction of the plane of shear with K_2; S, the shear strain value.

2. Twinning is one of important deformation modes in commercial-purity titanium during cyclic loading, and the quantitative relations of twin fraction versus strain amplitude and cyclic number were measured and proposed.

3. Dislocation structures in commercial-purity titanium were observed by TEM, and an evolution map of dislocation patterns versus strain and cyclic numbers was given. In combination with the evolution of microstructures, the effect of microstructures on the cyclic stress–strain response in commercial-purity titanium was discussed.

References

[1] H. Mughrabi, Mater. Sci. Eng. 33 (1978) 207–223.
[2] Z.S. Basinski, S.J. Basinski, Prog. Mater. Sci. 36 (1989) 89–148.
[3] O.B. Pedersen, K.V. Rasmussen, Acta Metall. 30 (1982) 57–65.
[4] P. Lukas, L. Kunz, Mater. Sci. Eng. A189 (1994) 1–7.
[5] D. Munz, Scr. Metall. 6 (1972) 815–819.
[6] D. Munz, Eng. Fract. Mech. 5 (1973) 353–364.
[7] R. Stevenston, J.F. Breedis, Acta Metall. 23 (1975) 1419–1429.
[8] J.I. Dickson, J. Ducher, A. Plumtrees, Metall. Trans. A 7 (1976) 1559–1565.
[9] N.E. Paton, W.A. Backonfen, Metall. Trans. A 1 (1970) 2839–2847.
[10] J.I. Dickson, L. Handfield, G. L'Esperance, Mater. Sci. Eng. 60 (1983) L3–L7.
[11] P.G. Partridge, Philos. Mag. 12 (1965) 1043–1054.
[12] N. Ecob, B. Ralph, The effect of grain size on the incidence of deformation twinning in a zinc-based alloy, in: N. Hansen et al. (Eds.), Deformation of Polycrystals Mechanisms and Microstructures, Int. Symp. Metals and Materials Science, 2nd Risø National Laboratory, Risø, Denmark, 1981, p. 177.
[13] W. Truszkouski, A. Latkowski, A. Dziodom, Stress–strain behavior and microstructure of polycrystalline α-Ti, in: N. Hansen et al. (eds), Deformation of Polycrystals Mechanisms and Microstructures, Int. Symp. Metals and Materials Science, 2nd Risø National Laboratory, Risø, Denmark, 1981, p. 205.
[14] K. Takao, K. Kusukawa, Mater. Sci. Eng. A213 (1996) 81–85.
[15] H.C. Gu, H.F. Guo, S.F. Zhang, C. Laird, Mater. Sci. Eng. A188 (1994) 23–36.
[16] X.L. Tan, H.C. Gu, S.F. Zhang, C. Laird, Mater. Sci. Eng. A189 (1994) 77–84.
[17] X.L. Tan, H.C. Gu, Z.G. Wang, Mater. Sci. Eng. A196 (1995) 45–52.
[18] M.P. Biget, G. Saada, Philos. Mag. A 59 (1989) 747–757.
[19] S. Naka, A. Lasalmonie, J. Mater. Sci. 18 (1982) 2613–2617.
[20] S. Naka, A. Lasalmonie, Mater. Sci. Eng. 59 (1982) 19–24.
[21] Y. Minonishi, S. Morozumi, H. Yoshinaga, Scr. Metall. 19 (1985) 1241–1245.
[22] Y. Minonishi, S. Morozumi, H. Yoshinaga, Scr. Metall. 16 (1982) 427–430.
[23] H. Numakura, Y. Minonishi, M. Koiwa, Scr. Metall. 20 (1986) 1581–1586.
[24] L. Xiao, H.F. Guo, H.C. Gu, Cyclic deforamation twinning in pure titanium and zirconium, in: Oikawa et al. (Eds.), Strength of Materials, Japan Institute of Metals, Tokyo, 1994, p. 163.

[25] N. Munroe, X.L. Tan, H.C. Gu, Scr. Mater. 36 (1997) 1383–1386.
[26] L. Xiao, H.C. Gu, Metall. Trans. 28 (1997) 1021–1033.
[27] C. Laird, P. Charsley, H. Mughrabi, Mater. Sci. Eng. 81 (1986) 433–450.
[28] P. Neumann, Mater. Sci. Eng. 81 (1986) 465–476.